Innovative Analysis Topics

Plenary Lecture: Abstract, Slides and Video
Rigid mechanics and its role in nonlinear structural analysis
Yeong Bin YANG (National Taiwan University)

The stability of plane shape under bending of elastically-plastic finite rigidity tendons, having non-symmetrical cross-section
Oleksandr SHYMANOVSKYI, Valeryi SHALYNSKYI (V. Shimanovsky UkrRDIsteelconstruction)*

Internal forces and displacements in polynomial-shaped arches
Lazaro GIMENA, Pedro GONZAGA, Faustino GIMENA (Public University of Navarre)*

Decision of initial shape and stress from equilibrium shape by structural analysis based on condition for existence of solution
Tetsu-Yuki TANAMI

Mistakes and paradoxes in solutions of spatial, geometrically nonlinear problems and equilibrium stability problems
Anatoly V. PERELMUTER (SCAD Soft), Vladimir I. SLIVKER (JSC Giprostroymost)*

For multiple-author papers:
Contact author designated by *
Presenting author designated by underscore

Proceedings of the 6th International Conference on
Computation of Shell and Spatial Structures
IASS-IACM 2008: "Spanning Nano to Mega"
28-31 May 2008, Cornell University, Ithaca, NY, USA
John F. ABEL and J. Robert COOKE (eds.)

Rigid mechanics and its role in nonlinear structural analysis

Y. B. YANG*

*Department of Civil Engineering, National Taiwan University
Taipei, Taiwan 10617
E-mail: ybyang@ntu.edu.tw

Abstract

In the nonlinear analysis of elastic structures, the displacement increments generated at each incremental step can be decomposed into two components as the *rigid displacements* and *natural deformations*. Based on the updated Lagrangian (UL) formulation, the geometric stiffness matrix $[k_g]$ is derived for a 3D *rigid beam element* from the virtual work equation using a rigid displacement field. Further, by treating the three-node triangular plate element (TPE) as the composition of three rigid beams lying along the three sides, the $[k_g]$ matrix for the TPE can be assembled from those of the rigid beams. The idea for the UL-type incremental-iterative nonlinear analysis is that if the rigid rotation effects are fully taken into account at each stage of analysis, then the remaining effects of natural deformations can be treated using the small-deformation linearized theory. The present approach is featured by the fact that the formulation is *simple*, the expressions are *explicit*, and *all* member actions are considered in the stiffness matrices. The robustness of the procedure has been demonstrated in the solution of several problems involving the postbuckling response in previous papers by the author.

1. Introduction

In the past half a century, great advances have been made in nonlinear structural analysis. A partial review of related previous works can be found in Ref. [1], in which a total of 122 papers up to 2002 were cited. Based on the updated Lagrangian (UL) formulation, the purpose of this paper is to present a *conceptually simple*, but *procedurally robust*, incremental-iterative approach for the nonlinear analysis of elastic structures, by taking advantage of the different properties of each phase of the analysis [2,3].

For an incremental-iterative nonlinear analysis, two typical phases can be identified, i.e., the *predictor* and *corrector* phases. The *predictor* relates to solution of the structural displacement increments for given load increments based on the incremental structural equation, and the *corrector* is concerned with recovery of the force increments from the displacement increments for each element and the updating of the element forces [4]. The predictor affects only the speed of convergence of iteration, which therefore is allowed to be approximate to the extent that the direction of iteration is not midguided. In contrast, the corrector governs primarily the accuracy of solution, which should thus be made as accurate as possible. A common understanding is that if the corrector is not accurate anough, then the unbalanced forces calculated will be incorrect and the iterations performed to remove the unbalanced forces will be meaningless.

2. Logistics of incremental-iterative scheme

In nonlinear analysis of structures, we are faced with solution of equations of equilibrium of the incremental form, as given below:

$$[K]\{\Delta U\} = \{\Delta P\} \tag{1}$$

where $[K]$ is the tangent stiffness matrix, $\{\Delta U\}$ the displacement increments to be solved, and $\{\Delta P\}$ the load increments applied on the structure for the current incremental step. As for the incremental-iterative analysis, a schematic diagram of the mechanism involved is given in Figure 1. The slope *ab* represents the tangent stiffness of the structure used in the predictor for computing the displacement increments $\{\Delta U\}$, given the load increment $\{\Delta P\} = \{^2P\} - \{^1P\}$. Clearly, a convergent solution can always be obtained, regardless of whether the stiffness

matrix (i.e., the slope) is updated or not, as indicated in the figure. In fact, this phase affects only the direction of iteration or the number of iterations, but *not* the accuracy of solution.

In Figure 1, the segment *cd* represents the initial forces existing on each element, *de* the force increments generated during the increment, and *be* the unbalanced forces. Both the updating of initial forces, as represented by segment *de*, and the calculation of force increments, as represented by segment *be*, are part of the *corrector* phase. Clearly, the corrector must be accurate enough for the unbalanced forces to be correct. This is the logistics for performing an efficient incremental-iterative nonlinear analysis.

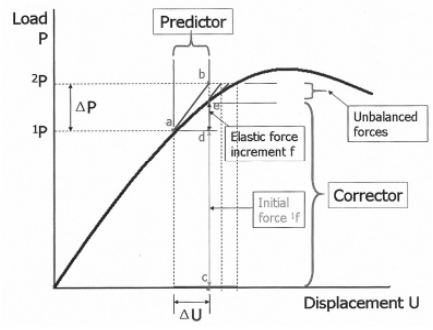

Figure 1: Idea of incremental-iterative analysis

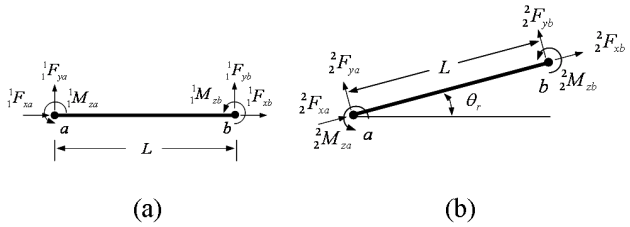

Figure 2: Initially stressed 2D beam: (a) before rigid rotation, (b) after rigid rotation

3. Rigid body rule

The rigid body rule is an important property that should be obeyed at all times in an incremental-iterative analysis, especially in the predictor and corrector phases. This rule requires that all the initial forces acting on an element should remain unchanged in magnitude and rotate following the rigid rotation. The result is the preservation of equilibrium of the element in the rotated position, as illustrated in Figure 2 [5,6].

4. Conventional finite element formulation

Based on the updated Lagrangian (UL) formulation, the virtual work equation for a finite element at C_2 but with reference to C_1 can be given in a linearized sense as [6]:

$$\int_V C_{ijkl}\,{}_1e_{kl}\delta\,{}_1e_{ij}dV + \int_V {}^1\tau_{ij}\delta\,{}_1\eta_{ij}dV = {}^2_1R - {}^1_1R \tag{2}$$

in which the first and second terms denote the strain energy and potential energy, respectively, V = volume, C_{ijkl} = constitutive coefficients, and ${}^1\tau_{ij}$ = Cauchy stresses of the element at C_1, δ = variation of the quantity following, and ${}_1e_{ij}$ and ${}_1\eta_{ij}$ = linear and nonlinear components of the strain increments with reference to C_1,

$${}_1e_{ij} = \frac{1}{2}\left(\frac{\partial u_i}{\partial x_j} + \frac{\partial u_j}{\partial x_i}\right), \quad {}_1\eta_{ij} = \frac{1}{2}\left(\frac{\partial u_k}{\partial x_i}\frac{\partial u_k}{\partial x_j}\right) \tag{3a,b}$$

where u_i = displacement increments and x_i = coordinates of the element at C_1. The external virtual works ${}^2_1R$ and ${}^1_1R$ at C_2 and C_1, respectively, can be related to the nodal loads $\left\{{}^2_1f\right\}$ and $\left\{{}^1_1f\right\}$ as

$${}^2_1R = \left\{\delta u\right\}^T\left\{{}^2_1f\right\}, \quad {}^1_1R = \left\{\delta u\right\}^T\left\{{}^1_1f\right\} \tag{4}$$

For a 3D beam element (Figure 3), the virtual work equation in Eq. (2) can be transformed into an *incremental stiffness equation* for the element from C_1 to C_2 as [6]

$$\left(\left[k_e\right]+\left[k_g\right]\right)\left\{u\right\} = \left\{{}^2_1f\right\} - \left\{{}^1_1f\right\} \tag{5}$$

where $\{u\}$ = displacement increments of the element. The *linear stiffness matrix* $[k_e]$ and *geometric stiffness matrix* $[k_g]$ can be derived as

$$\delta U = \int_V C_{ijkl}\,{}_1e_{kl}\delta\,{}_1e_{ij}dV = \left\{\delta u\right\}^T\left[k_e\right]\left\{u\right\}, \quad \delta V = \int_V {}^1\tau_{ij}\delta\,{}_1\eta_{ij}dV = \left\{\delta u\right\}^T\left[k_g\right]\left\{u\right\} \tag{6a,b}$$

By assembling Eq. (5) over all elements of a structure, we can obtain the structural equation as given in Eq. (1). In this study, we shall highlight that by choosing a robust incremental-iterative scheme, the use of the linear

stiffness matrix $[k_e]$, plus a *rigid-body qualified* geometric stiffness matrix $[k_g]$, is sufficient for solving a wide range of nonlinear problems.

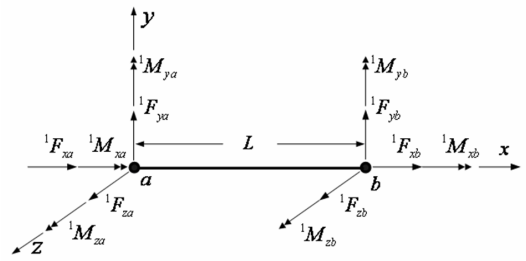

Figure 3: Three-dimensional beam element

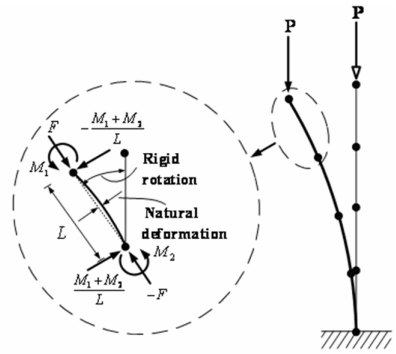

Figure 4: Rigid rotation and natural deformation

5. Concept of rigid rotation and rigid beam element

The displacements $\{u\}$ of each element of a structure in each incremental step can be decomposed into two parts as the *natural deformations* $\{u\}_n$ and *rigid displacements* $\{u\}_r$. In general, the *rigid displacements* constitute a great portion of the incremental displacements of each element (which are initially stressed) of the structure. In comparison, the magnitude of the *natural deformations* is relatively small for structures that are represented by a sufficient number of elements. Such a characteristic can be appreciated from the buckling of the cantilever shown in Figure 4.

For a rigid displacement field, the axial, twisting, and rotational displacements are constant, and the lateral displacements are linear, subjected to the constraints for the two ends that make the beam behave as a rigid or non-deformable body [2,3]. For this case, the strain energy in Eq. (6a) simply vanishes, i.e., $\delta U = 0$. One can derive from the potential energy term in Eq. (6b) a geometric stiffness matrix $[k_g]$ that is fully compatible with the rigid body rule. In Refs. [2,3], such a geometric stiffness matrix $[k_g]$ has been referred to as the stiffness matrix for the *rigid beam element*. One advantage with such an element is that it can be derived in a easy way and given in explicit form, while all member actions are duly taken into account.

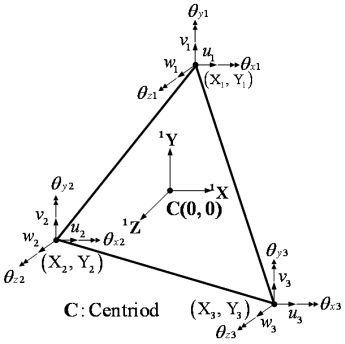

Figure 5: Three-node triangular plate element

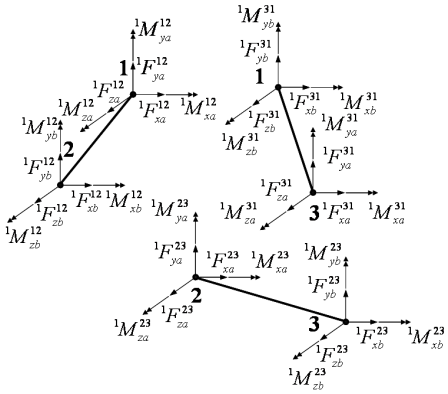

Figure 6: Forces and moments acting on each element

6. Triangular plate element (TPE) for plate and shell analysis

For the three-node *triangular plate element* (TPE) shown in Figure 5, there are three translational and three rotational DOFs at each node, thereby making each side of the element compatible with the 12-DOF beam element derived above. As far as the *rigid body behavior* of an element is concerned, only the *initial forces* acting on the element and the *external shape* of the element need to be considered. The elastic properties that are essential to the deformation of the element, such as Young's modulus, cross-sectional area and moments of

inertia, can be totally ignored. Based on such an idea, the rigid behavior of the TPE can be simulated as if it is composed of three rigid beams lying along the three sides of the element, as shown in Figure 6. It is by this concept that the geometric stiffness matrix $[k_g]$ for the rigid TPE was derived [3], which also appears to be explicit in form.

7. Stiffness matrices used in the predictor and corrector

As was pointed out previously, the structural stiffness matrix $[K]$ used in the predictor need *not* be exact and can be *approximate* in some sense, but must be accurate enough not to misguide the *direction of iteration* [7]. Such a point allows us to be released from the burden of deriving highly nonlinear elements, as conventionally attempted. It has been demonstrated in Refs. [2,3] that all we need for the predictor of an incremental-iterative analysis is the *linear stiffness matrix* $[k_e]$, made available from the linear theory, and the *geometric stiffness matrix* $[k_g]$ derived for the rigid element, for its qualification by the rigid body rule.

The *corrector* is concerned with recovery of the force increments $\{f\}$ from the displacement increments $\{u\}$ for each element and the updating of element forces at the end of the incremental step. For the case where each incremental step can be regarded as *small*, which is the case encountered by most nonlinear analysis, the element force increments $\{f\}$ can be computed with a sufficient level of accuracy using only the *linear stiffness matrix* $[k_e]$, and the initial nodal forces $\{{}^1f\}$ can be updated using the *rigid body rule* mentioned above. Clearly, the amount of computation involved in this phase is greatly reduced compared with the conventional approaches.

8. Concluding remarks

We have demonstrated that the geometric stiffness matrices can be derived for the 3D rigid beam element and rigid triangular plate element (TPE). It should be noted that in assembling the element stiffness matrices to form the structural matrix, joint equilibrium conditions should be established in the rotated position, as was described in Refs. [3,6], to account the effect of nodal moments undergoing rotations. In solving the postbuckling behaviors of structures using the prediction/corrector concept presented above, along with the rigid element and rigid body rule, it is essential that a reliable solution scheme be used. The scheme that has been demonstrated to be quite powerful is the generalized displacement control (GDC) method proposed in Ref. [8]. The applicability of the present procedure has been demonstrated in the solution of a number of nonlinear problems [2,3].

Acknowledgement

The research reported herein has been sponsored in part by the ROC National Science Council through a series of research projects to the author, including the one with grant No. 81-0410-E002-05.

References

[1] Yang YB, Yau JD, Leu LJ. Recent developments on geometrically nonlinear and postbuckling analysis of framed structures. *Applied Mechanics Reviews*, 2003; **56**(4): 431-449.

[2] Yang YB, Lin SP, Leu LJ. Solution strategy and rigid element for nonlinear analysis of elastic structures based on updated Lagrangian formulation. *Engineering Structures* 2007; **29**: 1189-1200.

[3] Yang YB, Lin SP, Chen, CS. Rigid body concept for geometric nonlinear analysis of 3D frames, plates and shells based on the updated Lagrangian formulation. *Computer Methods in Applied Mechanics and Engineering* 2007; **196**: 1178-1192.

[4] Yang YB, Leu LJ. Force recovery procedures in nonlinear analysis. *Computers and Structures* 1991; **41**(6): 1255-1261.

[5] Yang YB, Chiou HT. Rigid body motion test for nonlinear analysis with beam elements. *Journal of Engineering Mechanics* ASCE 1987; **113** (9):1404-1419.

[6] Yang YB, Kuo SR. *Theory and Analysis of Nonlinear Framed Structures* 1994; Prentice Hall, Englewood Cliffs, N.J.

[7] Kuo SR, Yang YB. Tracing postbuckling paths of structures containing multi loops. *International Journal for Numerical Methods in Engineering* 1995; **38**(23): 4053-4075.

[8] Yang YB, and Shieh MS, Solution method for nonlinear problems with multiple critical points. *AIAA Journal* 1990; **28**(12): 2110-2116.

Proceedings of the 6th International Conference on
Computation of Shell and Spatial Structures
IASS-IACM 2008: "Spanning Nano to Mega"
28-31 May 2008, Cornell University, Ithaca, NY, USA
John F. ABEL and J. Robert COOKE (eds.)

The stability of plane shape under bending of elastically-plastic finite rigidity tendons, having non-symmetrical cross-section

Oleksandr SHYMANOVSKYI*, Valeryi SHALYNSKYI

*Chairman of the Board "V. Shimanovsky Ukrainian Research and Design Institute of Steel Construction",
Dr. Sc. (Eng.), Professor, Honored Worker of Science and Engineering of Ukraine,
Academician of the Ukrainian Academy of Construction, Member of IASS
Ukraine, 02660, Kyiv, Vyzvolyteliv Prospect, 1
niipsk@webber.kyiv.ua

Abstract

The stability of plane shape under bending of elastically plastic finite rigidity tendons having non-symmetrical cross section, such as tee and channel profiles provided with vertical and horizontal web is under consideration.. The principal resolving equations of the problem are given, obtained on the basis of plastic flow theory with the aid energetic stability criterion in the form of Lagrange-Dirihle are presented. The results of investigations being made are described. The relationship curves of angle of slope value at separation border from parameter, featuring a relative height of elastic core of the cross section are highlighted .The peculiarities during the tendons behavior having tee and channel type cross section as compared with tendons having rectangular and I-section cross section were analyzed as well.

Problem definition

When operated the finite rigidity tendons outside elasticity limits along its length and simultaneously with elastic portions the regions are developed, covered by plastic deformations. That's why the potential energy of tendon under deformation in the case of its stability loss of plane bending shape will be composed of the energy sum at elastic and plastic portions. The potential energy of elastic portions under deformation may be determined according to formula:

$$W = \frac{1}{2}\int_{l_{yn.}} \left[EI_{\omega}(\theta'')^2 + GI_d(\theta')^2 + EI_z(v'')^2 \right] dx, \tag{1}$$

where EI_{ω}, GI_d, EI_z – sectorial torsion and flexural rigidities of tendon's cross section correspondingly ; v – displacements of cross sections in horizontal plane ; θ – angle of rotation of cross sections.

For plastic portions the expression of potential energy under deformation has the following view: (Shymanovskyi and Ogloblya [1])

$$W = \frac{1}{2}\int_{l_{yn.}} \left[EI^*_{\omega}(\theta'')^2 + GI_d(\theta')^2 + EI^*_z(v'')^2 \right] dx, \tag{2}$$

where EI^*_{ω} and EI^*_z – reduced sectorial and flexural rigidity of the cross section correspondingly.

It has been taken into consideration in (2) that in the case of stability loss of plane bending shape some part of tendon's section will be loaded and another part will be unloaded. Therefore, it is necessary to define the position of demarcation line at zones of loading and unloading.

Let's consider tee cross section of the tendon (fig. 1). In doing so we'll keep in mind that its dimensions are within the limits of relationships in the range of metal rolled stock.

In the event of one-way or two-way ductility the position of demarcation lines at zones of loading and unloading *m - m* in cross section may be found with the use of known assumption that during loss of the plane shape of strain the displacements of tendon in vertical plane are absent.

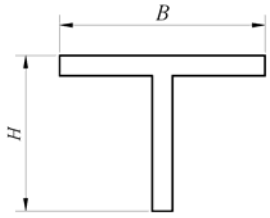

Fig. 1. Tee cross section of the tendon

Assuming for definiteness sake that in the case of one-way ductility the loading takes place in zone $F'_{пл}$, and unloading – in zone $F''_{пл}$, can be obtained

$$\left(I_y^{yn} + I''_y\right)\rho'' - I''_{yz}\,\nu'' = 0, \tag{3}$$

where I_y^{yn} and I''_y – moments of inertia of elastic core and unloading zone correspondingly $F''_{пл}$; I''_{yz} – product of inertia at unloading zone $F''_{пл}$; ρ'' and ν'' – curvatures of the tendon in vertical and horizontal planes correspondingly; *y* and *z* –main central axes of the tendon's cross section.

In the event of two-way ductility and taking into account that loading takes place at zones $F'_{пл}$ and $F''''_{пл}$, and unloading – at zones $F''_{пл}$ and $F'''_{пл}$, instead of relationship (3) we have:

$$\left(I_y^{yn} + I''_y + I'''_y\right)\rho'' - (I''_{yz} + I'''_{yz})\nu'' = 0\,. \tag{4}$$

Substitution of meanings conforming to tee section I_y^{yn}, I''_y, I''_{yz} for relationship (3) after reduction of similar members leads to equationпосле, characterizing the position of demarcation line for tee cross section under one-way ductility

$$A_1\omega_1^2 + A_2\omega_1 + A_3 = 0, \tag{5}$$

where $A_1 = 3\left(\zeta_1^4 - 4\alpha\zeta_1^3 + 4\alpha^2\zeta_1^2 + 4\alpha\eta_1 - 1\right)$;
$A_2 = 16bd^{-1}\left[\eta_2^3 - \eta_c^3\right] + 8\left[\zeta_1^3 - 3\alpha\zeta_1^2 + 3\alpha^2\zeta_1 + 3\alpha\eta_1 + 2\left(\eta_1^3 + \eta_c^3\right) - 1\right]$; $A_3 = 6\left(\zeta_1^2 - 2\alpha\zeta_1 - 2\eta_1 + 1\right)$.

Here the function $\omega_1 = ectg\varphi / d$, is introduced, determining the position of demarcation line unambiguously along with acceptance of the following designations $\eta_1 = h_1 / e$; $\eta_2 = h_2 / e$; $\eta_c = h_c / e$, $\zeta_1 = \xi_1 / e$; $\zeta_2 = \xi_2 / e$, $\alpha = 1 - \eta_1$.

After similar substitution of corresponding meanings I_y^{yn}, I''_y, I'''_y, I''_{yz}, I'''_{yz} for relationship (4) and reduced appropriate members we may find the equation, specifying the position of demarcation line for tee cross section under two-way ductility

$$B_1\omega_1^2 + B_2\omega_1 + B_3 = 0, \tag{6}$$

where $B_1 = 3\left[\left(\zeta_2^4 + \zeta_1^4\right) + 4\left(\zeta_2^3 - \zeta_1^3\right)\alpha + 4\left(\zeta_2^2 + \zeta_1^2\right)\alpha^2 - \left(\eta_1^2 - \eta_2^2 + 2\alpha\right)^2 + 2\left(\eta_1^2 - \eta_2^2 + 1\right)\right]$;
$B_2 = 8bd^{-1}\left[\zeta_2^3 + 3\alpha\zeta_2^2 + 3\alpha^2\zeta_2 + \alpha^3 - 2\eta_c^3 + \eta_2^3\right] + 8\left[\zeta_1^3 - 3\alpha\zeta_1^2 + 3\alpha^2\zeta_1 - \alpha^3 + \ + \eta_1^3 + 2\eta_c^3\right]$;
$B_3 = 6b^2d^{-2}\left[\zeta_2^2 + 2\alpha\zeta_2 + \alpha^2 - \eta_2^2\right] + 6\left[\zeta_1^2 - 2\alpha\zeta_1 + \alpha^2 - \eta_1^2\right]$.

Let's analyze cross section of the tendon in the form of channel with vertical web (fig. 2), when its dimensions are within the limits of relationships in the range of metal rolled stock. In channel-type cross section the finite rigidity tendons when operated beyond the elasticity limits also can be realized in two cases of ductility, in

particular in one-way and two-way versions. In the event of one-way ductility it is possible to obtain the equation through the use of expression (3), characterizing the position of demarcation line

$$C_1\omega_2^2 + C_2\omega_2 + C_3 = 0, \tag{7}$$

where $C_1 = 3\left(\zeta_1^4 - 4\alpha\zeta_1^3 + 4\alpha^2\zeta_1^2 - 4\alpha^2 + 4\alpha - 1\right)$;
$C_2 = 32b_1^{-1}d\eta_c^3 + 8b_1^{-1}b_2\left(\zeta_1^3 - 3\alpha\zeta_1^2 + 3\alpha^2\zeta_1 - \alpha^3 + \eta^3 - 2\eta_c^3\right) + 16\left(\eta^3 - \eta_c^3\right)$; $C_3 = 6\left(\zeta_1^2 - 2\alpha\zeta_1 + 2\alpha - 1\right)$.

Here the function $\omega_2 = ectg\varphi / b_1$, is introduced, determining the position of demarcation line in this particular case.

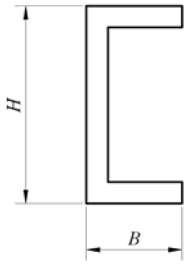

Fig. 2. Cross section of the tendon using channel with vertical web

In the event of two-way ductility in channel-type cross section with vertical web we may obtain expression for determination of the position of demarcation line with application of equation (4)

$$D_1\omega_2^2 + D_2\omega_2 + D_3 = 0, \tag{8}$$

where $D_1 = 3\left[\zeta_1^4 + \zeta_2^4 - 4\alpha\left(\zeta_1^3 - \zeta_2^3\right) + 4\alpha^2\left(\zeta_1^2 + \zeta_2^2\right) - 8\alpha^2 + 8\alpha - 2\right]$;
$D_2 = 32b_1^{-1}d\eta_c^3 + 8b_1^{-1}b_2\left(\zeta_1^3 - 3\alpha\zeta_1^2 + 3\alpha^2\zeta_1 - \alpha^3 + \eta^3 - 2\eta_c^3\right) + 8\left(\zeta_2^3 + 3\alpha\zeta_2^2 + 3\alpha^2\zeta_2 + \alpha^3 + \eta^3 - 2\eta_c^3\right)$;
$D_3 = 6b_1^{-2}b_2^2\left(\zeta_2^2 + 2\alpha\zeta_2 - \beta\right) + 6\left(\zeta_1^2 - 2\alpha\zeta_1 - \beta\right)$.

During consideration of cross section of the tendon using channel with horizontal web (fig. 3), when its dimensions are within the limits in range of rolled metal stock it should be noted that here two cases of ductility are realized also, in particular in one-way and two0way versions. The equation, specifying the position of demarcation line in the case of one-way ductility can be obtained with the aid of expression (3)

$$E_1\omega_3 + E_2 = 0\,, \tag{9}$$

where $E_1 = 8\left[\zeta_2^3 + 3\alpha\zeta_2^2 + 3\alpha^2\zeta_2 + \alpha^3 + 2\eta_1^3 + \eta_2^3\right] - 8h_c h^{-1}\left[\zeta_2^3 + 3\alpha\zeta_2^2 + 3\alpha^2\zeta_2 + \alpha^3 + 2\left(\eta_1 - 2\eta_d\right)^3 + \eta_2^3\right]$;
$E_2 = 6\left(1 - h_c^2h^{-2}\right)\left(\zeta_2^2 + 2\alpha\zeta_2 + \alpha^2 - \eta_2^2\right)$.

Here the function $\omega_3 = ectg\varphi / h$, is introduced, which defines the position of demarcation line for a given case. In this event $\eta_d = d / e$.

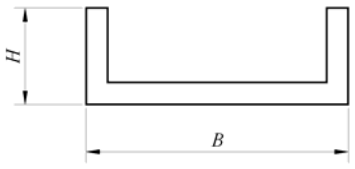

Fig. 3. Cross section of the tendon using channel with horizontal web

In the event of two-way ductility in channel-type cross section with horizontal web we may obtain equation for determination of the position of demarcation line in zones of loading and unloading, so *m – m*, may be regarded as

$$F_1\omega_3^2 + F_2\omega_3 + F_3 = 0\,, \tag{10}$$

where $F_1 = 3\left(\zeta_1^4 - 4\alpha\zeta_1^3 + 4\alpha^2\zeta_1^2 - 4\alpha^2 + 4\alpha - 1\right)$;

$F_2 = 8\left[\zeta_1^3 + \zeta_2^3 - 3\alpha\left(\zeta_1^2 - \zeta_2^2\right) + 3\alpha^2\left(\zeta_1 + \zeta_2\right) + \eta_1^3 + \eta_2^3\right] - 8h_c h^{-1}\left[\zeta_2^3 + 3\alpha\zeta_2^2 + 3\alpha^2\zeta_2 + \alpha^3 + \eta_2^3 + 2\left(\eta_1 - 2\eta_d\right)^3\right]$;

$F_3 = 6\left[\zeta_1^2 + \zeta_2^2 - 2\alpha\left(\zeta_1 - \zeta_2\right) + \alpha^3 - \eta_1 - \eta_2^2\right] - 6h_c^2 h^{-2}\left[\zeta_2^2 + 2\alpha\zeta_2 + \alpha^2 - \eta_2^2\right]$.

If to consider relationships (5) and (6) it can be tolerated that $e = h_1$, in (7) and (8) – that $e = h$, and in (9) and (10) – that $e = b_1$, then we come to the case of the stability loss in plane shape during bending of elastic and plastic beams. In such cases the function $\omega(\zeta)$, is under analysis, when parameter ζ defines a relative height of elastic core part in cross section of the beam, located between neutral axis and plastic region. The similar problem was reviewed in details for rectangular cross section for the first time by L. Kachanov (Kachanov [2]). In such a manner, the problem regarding the stability loss of plane shape during bending of elastically plastic beams may be considered as a specific case of the problem under review, namely the stability loss of plane shape during bending of elastically plastic finite rigidity tendons.

The numerical results

In the process of consideration of tee beam behavior outside elasticity limits under stability loss of plane shape during bending it is possible to notice that function ω, relationship curve, describing value of slope of demarcation line as regards a relative height of elastic core part ζ in the case of one-way ductility in the web (in pure bending the ductility zone appears in the web only) approaches to parabolic form. This form of curve preserves up to the moment when distinction line passes across the lower horizontal edge of the web. In the case its slope is increased to the point where it begins to cross the lateral vertical edge of the web, so the curve may be changed into hyperbolic form. In this situation the slope of demarcation line is increased in ten times faster. Thereafter two-way ductility of the cross section will take place and an increase of the slope becomes even more evident.

The graph of function ω, relationship, which defines value of slope of demarcation line depending on parameter ζ in beams having cross section made of channel with vertical web has the form, peculiar to rectangular cross section. The only distinction is that in beams with channel-type cross section under increase of areas in regions of ductility the slope of demarcation line grows remarkably quicker as compared with cases of rectangular cross sections. In the process of detailed investigation of channel-type beam (for example having cross section 5П) outside the elasticity limits under the loss of stability it is possible to notice that its slope of demarcation line increases approximately by 2,5 times faster, than in beams having rectangular cross section. When ω_2 = 0,95 the flanges of this channel become completely plastic.

On the basis of analysis of channel-type beam behavior with horizontal web it follows that the relationship curve $\omega_3(\zeta)$ under one-way ductility in the flanges (in pure bending the ductility zone appears firstly in the web only) very close to parabolic form. When ζ = 1 in curves the inflection point in graph is present. From this time on the two-way ductility begins and the slope of demarcation line starts to increase apparently faster. At the same moment its relationship approaches to hyperbolic form. It must be emphasized that the relationship of curve $\omega(\zeta)$ for rectangular cross section is close to hyperbolic form too, but the slope increases faster in the event of cross section with channel having horizontal web. Specifically for channel 5П the slope of demarcation line increases approximately in double-quick time than for rectangular section. When ω = 0,65 the given channel web becomes completely plastic.

References

[1] Shymanovskyi A., Ogloblya A. The theory and calculation of load-carrying elements used in large-span spatial structures. Stal Publishing House: Kiev, 2002.

[2] Kachanov L. The basic principles of theory of plasticity. Gostekhizdat Publishing House: Moscow, 1956.

Proceedings of the 6th International Conference on
Computation of Shell and Spatial Structures
IASS-IACM 2008: "Spanning Nano to Mega"
28-31 May 2008, Cornell University, Ithaca, NY, USA
John F. ABEL and J. Robert COOKE (eds.)

Internal forces and displacements in polynomial-shaped arches

Lazaro GIMENA*, Pedro GONZAGA, Faustino GIMENA

*Public University of Navarre
Department of Projects Engineering, Campus Arrosadia C.P. 31006, Pamplona, Navarre, Spain.
Tel.: +34 948 169233; fax: +34 948 169644.
E-mail: lazaro.gimena@unavarra.es

Abstract

This paper deals with 2D-curved beam arches with polynomial free geometry. The problem is approach differentially and equations that govern its mechanical behavior are expressed. The obtained system of twelve linear ordinary differential equations is solved using either an analytical or a customized numerical method with boundary conditions. Expressions of the transfer and stiffness matrices can be derived directly. Functions and graphs of the different components of forces, moments, rotations and displacements are given. Examples of different polynomial-shaped arches are provided for verification.

1. Introduction

Since the first of last century, there exists much literature on structural analysis of curved beam elements, see for example Love [3] through Washizu [7]. Most of the authors approach this problem of twisted elements, expressing the functions in natural coordinates using the Frenet frame system of reference. These approaches to simulate the mechanical behavior of the problem, could be in meaning of virtual works and energy methods; in separate equations of equilibrium and kinematics; or in terms of a system of equations Yu *et al*. [8]. Particularly, the circular arch is a problem very spread in this field. Other types of curved arch element as parabola and helix have been considered Marquis *et al.* [4]. In the state of the art, the independent variable for curved beams has been the arc length *s* (naturally equations).

In this paper, the approach will be in function of the parameter *x* coordinate of the Cartesian reference system (non-naturally equations). A system of twelve differential equations is obtained and simulates the structural behavior of a twisted beam (Gimena *et al.* [2]). In special cases, this system is particularized, and a subsystem arises, to model the mechanical behavior of arches. Polynomial-shaped arches are studied in this research. Different results of internal forces and displacements for polynomial quadric degree arches are provided in graphs for comparison and verification purposes. Parabolic arch shape is optimal to transmit a vertical uniform distributed load as shown in the examples.

2. Equations of the curved beam

A curved beam is generated by a plane cross-section which centroid *P* sweeps normally through all the points of an axis line. The vector radius $\mathbf{r}=\mathbf{r}(s)$ expresses this curved line, where s (length of the arc) is the independent variable of the structural problem. The reference coordinate system used to represent the intervening known and unknown functions of the problem is the Frenet frame P_{tnb}. Its unit vectors tangent **t**, normal **n** and binormal **b** are: $\mathbf{t}=D\mathbf{r}$; $\mathbf{n}=D^2\mathbf{r}/|D^2\mathbf{r}|$; $\mathbf{b}=\mathbf{t}\wedge\mathbf{n}$; where $D=d/ds$ is the derivative with respect to the parameter *s*.
The Frenet-Serret equations (Struik [5]) describe the movement of the frame system along the axis line. These equations relate versors tangent, normal and binormal with their derivates with respect to the arc length and curvatures. In matricial form:

$$D\begin{bmatrix}\mathbf{t}\\ \mathbf{n}\\ \mathbf{b}\end{bmatrix}=\begin{bmatrix}0 & \chi(s) & 0\\ -\chi(s) & 0 & \tau(s)\\ 0 & -\tau(s) & 0\end{bmatrix}\begin{bmatrix}\mathbf{t}\\ \mathbf{n}\\ \mathbf{b}\end{bmatrix} \tag{1}$$

Where $\chi=\chi(s)$ and $\tau=\tau(s)$ are the flexure and torsion curvatures respectively, which represent the natural equations of the centroid line.

Assuming the habitual principles and hypotheses of the strength of materials (Timoshenko [6]) and considering the stresses associated with the normal cross-section (σ, τ_n, τ_b), the geometric characteristics of the section are: area $A(s)$, shearing coefficients $\alpha_n(s)$, $\alpha_{nb}(s)$, $\alpha_{bn}(s)$, $\alpha_b(s)$, and moments of inertia $I_t(s)$, $I_n(s)$, $I_b(s)$, $I_{nb}(s)$. Longitudinal $E(s)$ and transversal $G(s)$ elasticity moduli give the elastic condition of the material.

Applying the equilibrium law in forces, the following equation is obtained:

$$\begin{bmatrix} D & -\chi & 0 \\ \chi & D & -\tau \\ 0 & \tau & D \end{bmatrix} \begin{bmatrix} N \\ V_n \\ V_b \end{bmatrix} + \begin{bmatrix} q_t \\ q_n \\ q_b \end{bmatrix} = \begin{bmatrix} 0 \\ 0 \\ 0 \end{bmatrix} \tag{2}$$

Internal $\mathbf{V_t} = N\mathbf{t} + V_n\mathbf{n} + V_b\mathbf{b} = \int_A \sigma dA\mathbf{t} + \int_A \tau_n dA\mathbf{n} + \int_A \tau_b dA\mathbf{b}$ and load $\mathbf{q_t} = q_t\mathbf{t} + q_n\mathbf{n} + q_b\mathbf{b}$ forces.

The equation of moments is obtained applying the equilibrium law as well:

$$\begin{bmatrix} 0 & 0 & 0 \\ 0 & 0 & -1 \\ 0 & 1 & 0 \end{bmatrix} \begin{bmatrix} N \\ V_n \\ V_b \end{bmatrix} + \begin{bmatrix} D & -\chi & 0 \\ \chi & D & -\tau \\ 0 & \tau & D \end{bmatrix} \begin{bmatrix} T \\ M_n \\ M_b \end{bmatrix} + \begin{bmatrix} m_t \\ m_n \\ m_b \end{bmatrix} = \begin{bmatrix} 0 \\ 0 \\ 0 \end{bmatrix} \tag{3}$$

Internal $\mathbf{M_t} = T\mathbf{t} + M_n\mathbf{n} + M_b\mathbf{b} = \int_A (\tau_b n - \tau_n b) dA\mathbf{t} + \int_A \sigma b dA\mathbf{n} + \int_A \sigma n dA\mathbf{b}$ and load $\mathbf{m_t} = m_t\mathbf{t} + m_n\mathbf{n} + m_b\mathbf{b}$ moments.

Once the constitutive relations are defined, kinematics law relates the rotations and displacements:

$$\begin{bmatrix} -\frac{1}{GI_t} & 0 & 0 \\ 0 & -\frac{I_b}{E(I_nI_b - I_{nb}^2)} & -\frac{I_{nb}}{E(I_nI_b - I_{nb}^2)} \\ 0 & -\frac{I_{nb}}{E(I_nI_b - I_{nb}^2)} & -\frac{I_n}{E(I_nI_b - I_{nb}^2)} \end{bmatrix} \begin{bmatrix} T \\ M_n \\ M_b \end{bmatrix} + \begin{bmatrix} D & -\chi & 0 \\ \chi & D & -\tau \\ 0 & \tau & D \end{bmatrix} \begin{bmatrix} \theta_t \\ \theta_n \\ \theta_b \end{bmatrix} - \begin{bmatrix} \Theta_t \\ \Theta_n \\ \Theta_b \end{bmatrix} = \begin{bmatrix} 0 \\ 0 \\ 0 \end{bmatrix} \tag{4}$$

The rotations are given by the vector $\boldsymbol{\theta_t} = \theta_t\mathbf{t} + \theta_n\mathbf{n} + \theta_b\mathbf{b}$ and rotation load $\boldsymbol{\Theta_t} = \Theta_t\mathbf{t} + \Theta_n\mathbf{n} + \Theta_b\mathbf{b}$.

$$\begin{bmatrix} -\frac{1}{EA} & 0 & 0 \\ 0 & -\frac{\alpha_n}{GA} & -\frac{\alpha_{nb}}{GA} \\ 0 & -\frac{\alpha_{nb}}{GA} & -\frac{\alpha_b}{GA} \end{bmatrix} \begin{bmatrix} N \\ V_n \\ V_b \end{bmatrix} + \begin{bmatrix} 0 & 0 & 0 \\ 0 & 0 & -1 \\ 0 & 1 & 0 \end{bmatrix} \begin{bmatrix} \theta_t \\ \theta_n \\ \theta_b \end{bmatrix} + \begin{bmatrix} D & -\chi & 0 \\ \chi & D & -\tau \\ 0 & \tau & D \end{bmatrix} \begin{bmatrix} u \\ v \\ w \end{bmatrix} - \begin{bmatrix} \Delta_t \\ \Delta_n \\ \Delta_b \end{bmatrix} = \begin{bmatrix} 0 \\ 0 \\ 0 \end{bmatrix} \tag{5}$$

Where displacement components are denoted as $\boldsymbol{\delta_t} = u\mathbf{t} + v\mathbf{n} + w\mathbf{b}$ and displacement load $\boldsymbol{\Delta_t} = \Delta_t\mathbf{t} + \Delta_n\mathbf{n} + \Delta_b\mathbf{b}$.

Composing the unique system of linear ordinary differential equations which simulates the structural behavior of a curved beam element, next expression is reached (Gimena *et al.* [2]):

$$\begin{aligned}
& DN - \chi V_n + q_t = 0 \\
& \chi N + DV_n - \tau V_b + q_n = 0 \\
& \tau V_n + DV_b + q_b = 0 \\
& DT - \chi M_n + m_t = 0 \\
& -V_b + \chi T + DM_n - \tau M_b + m_n = 0 \\
& V_n + \tau M_n + DM_b + m_b = 0 \\
& -\frac{T}{GI_t} + D\theta_t - \chi\theta_n - \Theta_t = 0 \\
& -\frac{M_n I_b}{E\left[I_nI_b - I_{nb}^2\right]} - \frac{M_b I_{nb}}{E\left[I_nI_b - I_{nb}^2\right]} + \chi\theta_t + D\theta_n - \tau\theta_b - \Theta_n = 0 \\
& -\frac{M_n I_{nb}}{E\left[I_nI_b - I_{nb}^2\right]} - \frac{M_b I_n}{E\left[I_nI_b - I_{nb}^2\right]} + \tau\theta_n + D\theta_b - \Theta_b = 0 \\
& -\frac{N}{EA} + Du - \chi v - \Delta_t = 0 \\
& -\frac{\alpha_n V_n}{GA} - \frac{\alpha_{nb} V_b}{GA} - \theta_b + \chi u + Dv - \tau w - \Delta_n = 0 \\
& -\frac{\alpha_{bn} V_n}{GA} - \frac{\alpha_b V_b}{GA} + \theta_n + \tau v + Dw - \Delta_b = 0
\end{aligned} \tag{6}$$

Note the strict order of the twelve functions in the equation: forces produce moments; moments produce rotations and rotations produce displacements. All functions are interconnected. This arranged format has permitted to obtain directly numerical results and matrices expressions.

2.1 Polynomial arches

Let's consider a polynomial curve in the Cartesian plane. Its geometric explicit equation defining the shape is given by $y = p(x)$. The derivative of the arc length s with respect to the independent variable x is:

$$ds/dx = \sqrt{1+p'(x)^2} \tag{7}$$

The reference system used to annotate the intervening known and unknown functions is the Frenet frame. Their unit vectors tangent **t**, normal **n**, and binormal **b**, applying relation (7) are obtained in function of x:

$$\mathbf{t} = \left\{1/\sqrt{1+p'(x)^2}\,,\, p'(x)/\sqrt{1+p'(x)^2}\,,0\right\} \qquad \mathbf{n} = \left\{-p'(x)/\sqrt{1+p'(x)^2}\,,1/\sqrt{1+p'(x)^2}\,,0\right\} \qquad \mathbf{b} = \mathbf{z} \tag{8}$$

The natural equations of polynomial-shaped planar curve, are reduced to the expression of the flexion curvature $\chi=\chi(x)$, since torsion curvature is null $\tau=\tau(x)=0$.

$$\chi = p''(x)/\left[\sqrt{1+p'(x)^2}\right]^3 \tag{9}$$

In the special case that the cross section is symmetric, the product of inertia $I_{nb}(s)$ and the shearing coefficient $\alpha_{bn}(s)$ are null, and the system (6) can be decoupled in two subsystems, and the model is reduce to analyze the following expression:

$$\begin{aligned}
&\frac{dN}{dx} - \frac{p''(x)}{1+p'(x)^2}V_n + \sqrt{1+p'(x)^2}\,q_t = 0\\
&\frac{p''(x)}{1+p'(x)^2}N + \frac{dV_n}{dx} + \sqrt{1+p'(x)^2}\,q_n = 0\\
&\sqrt{1+p'(x)^2}V_n + \frac{dM_z}{dx} + \sqrt{1+p'(x)^2}\,m_z = 0\\
&-\sqrt{1+p'(x)^2}\frac{M_z}{EI_z} + \frac{d\theta_z}{dx} - \sqrt{1+p'(x)^2}\,\Theta_z = 0\\
&-\sqrt{1+p'(x)^2}\frac{N}{EA} + \frac{du}{dx} - \frac{p''(x)}{1+p'(x)^2}v - \sqrt{1+p'(x)^2}\,\Delta_t = 0\\
&-\sqrt{1+p'(x)^2}\frac{\alpha_n V_n}{GA} - \sqrt{1+p'(x)^2}\,\theta_z + \frac{p''(x)}{1+p'(x)^2}u + \frac{dv}{dx} - \sqrt{1+p'(x)^2}\,\Delta_n = 0
\end{aligned} \tag{10}$$

To obtain results of internal forces and displacements at any point of the polynomial curved beam, proper analytical or numerical methods for solving system of linear ordinary differential equations applied. Transfer and stiffness matrices can also be determined following procedures exposed in Gimena *et al.* [1].

3. Example. Polynomial symmetric shaped arches of quartic degree.

Five symmetric polynomial-shaped arches of quartic degree are presented with height f and span $2l$ (Figure 1). The section is constant and support is fixed-fixed, with vertical in projection udl of q=1 kN/m.

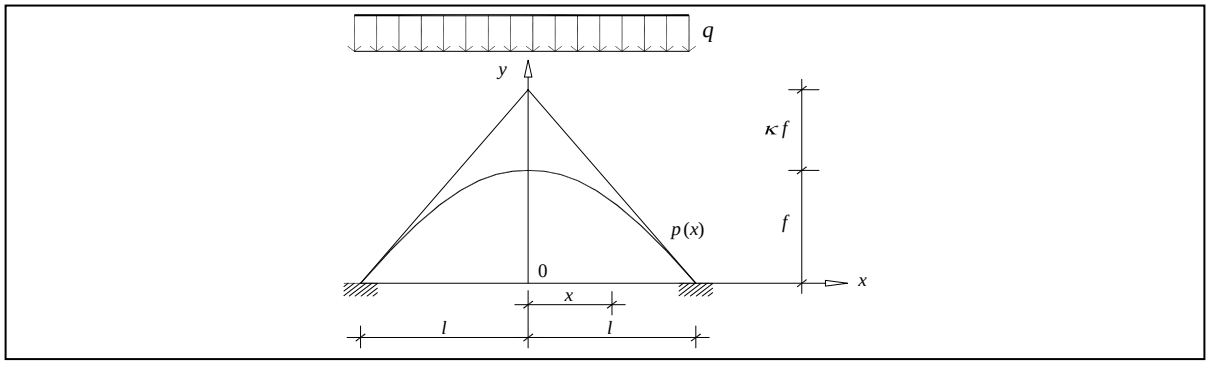

Figure 1. Polynomial-shaped arch.

The cartesian explicit expression for these arches is: $p(x) = f\,[2l^4 - (3-\kappa)\,l^2x^2 + (1-\kappa)\,x^4\,] / 2l^4$ where κ is a factor of the tangents at the extremes. Dimensions are : f=10m; l=10m and κ={0;0.5;1;1.5;2}. In these examples, he cross section is circular with diameter d=0.5m.

The geometric characteristics of the section are: $A = \pi d^2/4$, $I_n = I_b = \pi d^4/64$, $I_t = \pi d^4/32$. Shearing deformation is neglected, thus α_n=0, α_z=0. The elastic isotropic homogenous material has longitudinal $E = 3 \cdot 10^7$ kN/m^2 and transversal $G = 1{,}25 \cdot 10^7$ kN/m^2 moduli. Results are plotted in next figure 2:

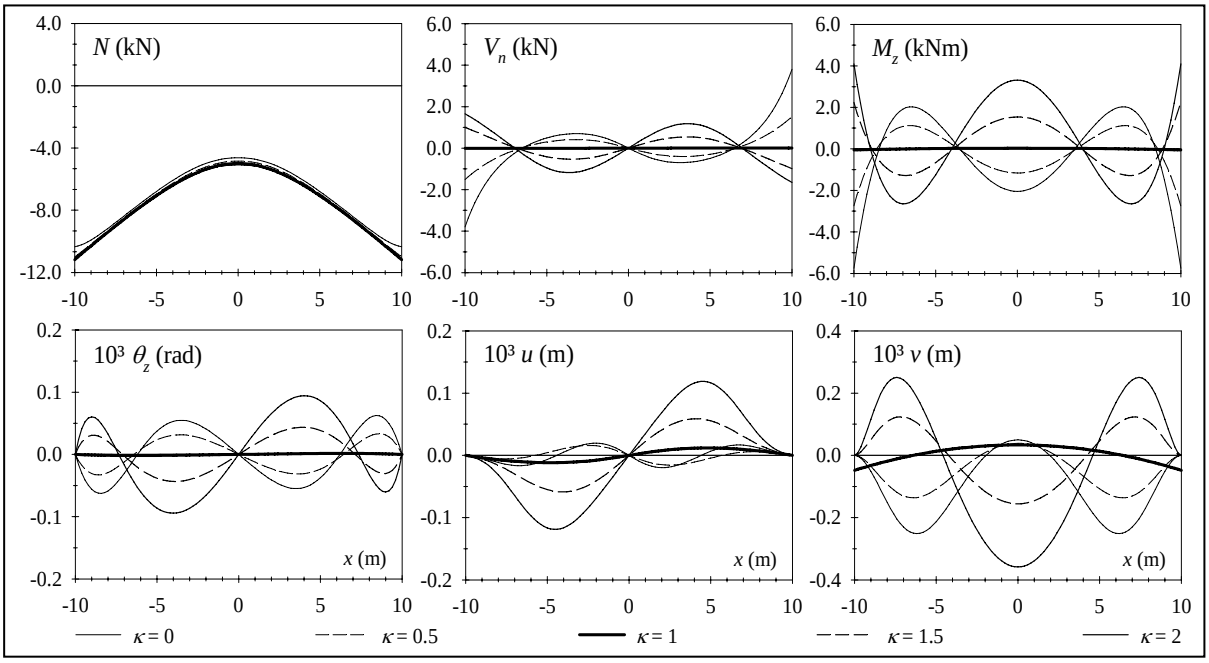

Figure 2. Internal forces and displacements in different polynomial arches. Comparison.

It can be distinguished that the parabola (κ=1) structurally behaves better than other arches, since its deflection, rotations, moments and shear effects are negligible. Its geometry is optimal for distributing the vertical load.

4. Conclusions

A differential system of twelve ordinary equations that models the structural behavior of a spatial curved beam is presented. This system is particularized for the calculus of polynomial-shaped arches. A 2D-curved beam can be approximated through polynomial functions, thus the procedure exposed is applicable. The set of equations could be solved analytically or numerically. Expressions of the transfer and stiffness matrices can be derived directly. The method permits the comparison of different type of arches. Accurate results of the components of forces, moments, rotations and displacements have been obtained and plotted. The interpretation of these results shows that the parabola is the optimal shape for transmitting a vertical uniform distributed load in projection.

References

[1] Gimena FN, Gonzaga P, Gimena L. New procedure to obtain the stiffness and transfer matrices of an elastic linear element. *16th Engineering Mechanics Conference: ASCE*. 2003.

[2] Gimena FN, Gonzaga P, Gimena L,. 3D-curved beam element with varying cross-sectional area under generalized loads. *Engineering Structures* 2008; **30**: 404-411.

[3] Love AEH. A Treatise on the mathematical theory of elasticity. New York: Dover; 1944.

[4] Marquis JP, Wang TM. Stiffness matrix of parabolic beam element. *Computer & Structures* 1989; **6**: 863–870.

[5] Struik DJ, Lectures on classical differential geometry. Addison-Wesley: Cambridge, 1950.

[6] Timoshenko S. Strength of materials. New York: D. Van Nostrand Company; 1957.

[7] Washizu K. Some considerations on a naturally curved and twisted slender beam. *Journal of Applied Mathematics and Physics*, 1964; **43(2)**: 111–116.

[8] Yu A, Fang M, Ma X. Theoretical research on naturally curved and twisted beams under complicated loads. *Computer & Structures* 2002; **80**: 2529-2536.

Proceedings of the 6th International Conference on
Computation of Shell and Spatial Structures
IASS-IACM 2008: "Spanning Nano to Mega"
28-31 May 2008, Cornell University, Ithaca, NY, USA
John F. ABEL and J. Robert COOKE (eds.)

Decision of initial shape and stress from equilibrium shape by structural analysis based on condition for existence of solution

Tetsu-Yuki TANAMI

Member of IASS
(Home) 2-13-8-103 Kugayama, Suginami-ku, Tokyo 168-0082, JAPAN
ttanami@aol.com

Abstract

A mixed-type finite deformation analysis is carried out with the situation where the equilibrium shape and the constant load are given. In this analysis, one unknown variable is the initial geometrical shape before loading. Another unknown is the variable which is necessary to specify the self-stress components existing in the given equilibrium shape. The analysis is supported by using the Moore-Penrose generalized inverse.

The solution forms of displacement method, stress method and mixed-type method, which are derived from the application of the Moore-Penrose generalized inverse to the structural analysis as small deformation problem, are also simply introduced to explain the ideas of the mixed-type analysis in this paper.

1. Introduction

Calculation of simultaneous system of linear equations in the conventional structural analysis is strongly depended on the mathematical condition of the regularity of the matrix, though the regularity condition is just an option to get solution. The point of using the Moore-Penrose generalized inverse in this paper is that we are not restricted by the regularity condition. Then the extent of the application of the analysis can cover any unstable structure with mechanism when the condition for the existence of a solution is satisfied. The ideas has been shown in Tanami [4,7,9] and roughly summarized in Tanami [2,3,5,6,8]. I can say as the result given from these research works that it might be possible to make up new approaches for getting more reasonable treatments of structural analysis in the field of shells and spatial structures.

In the conventional structural analysis, we have been considering that initial shape is deformed by the loading to satisfy the equilibrium condition as shown in figure 1, where the initial shape of Figure 1(a) is given as known. Then the equilibrium shape and the axial force existing in the deformed equilibrium shape of Figure 1(b) are unknowns.

(a) Initial geometrical shape (b) Equilibrium shape and axial forces

Figure 1: Usual finite deformation analysis

The situation is changed in this paper to fit in the actual sense where it is natural to think that the shape drawn by architect's side should become the real after the construction. Then the drawn shape is the equilibrium shape as shown in Figure 2(a) where it means that the equilibrium shape is known as constant. Then the initial shape is unknown together with the axial force as shown in Figures 2(b2) and 2(b1), respectively.

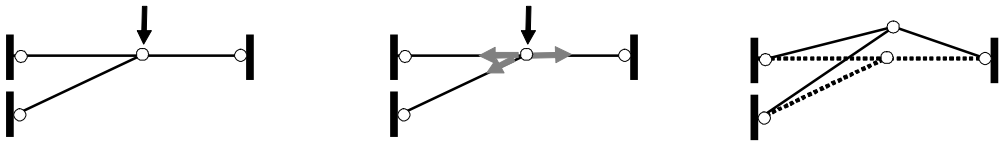

(a) Given equilibrium shape and the load (b1) Axial forces (b2) Initial geometrical shape by unloading

Figure 2: Finite deformation analysis in this paper

2. Mixed-type method

The derivation processes and the solution forms of displacement method, stress method and mixed-type method are simply summarized in this section by citing the papers in Tanami [4,7,9].

In the case of the small deformation analysis of truss structure, for instance, the compatibility equation, the constitutive equation and the equilibrium equation take the following forms, respectively,

$$\mathbf{A}\mathbf{u} = \boldsymbol{\varepsilon}, \quad \mathbf{E}\boldsymbol{\varepsilon} = \boldsymbol{\sigma}, \quad \mathbf{B}\boldsymbol{\sigma} = \mathbf{f} \qquad (1)(2)(3)$$

Note that there is the relation of $\mathbf{B}^{\mathbf{t}} = \mathbf{A}$. The matrix $\mathbf{A}$ with the size (m,n) is the transposed matrix of the matrix $\mathbf{B}$. Then the constitutive matrix $\mathbf{E}$ has the size (m,m). The vectors of $\boldsymbol{\varepsilon}$, $\mathbf{u}$, $\boldsymbol{\sigma}$ and $\mathbf{f}$ denote the change in length, the displacement, the axial force and the external constant load, respectively. From the equations (1), (2) and (3), the displacement is related with the external load in the form,

$$\mathbf{K}\mathbf{u} = \mathbf{f} \qquad (4)$$

Where the symbol $\mathbf{K}(=\mathbf{BEA})$ is the elastic stiffness matrix.

In the case of the displacement method, the equation of the problem and the solutions take the following forms,

$$\mathbf{K}\mathbf{u} = \mathbf{f} \quad \vdots \quad \mathbf{u} = \mathbf{K}^{-}\mathbf{f} + \left(\mathbf{I}_{\mathrm{n}} - \mathbf{K}^{-}\mathbf{K}\right)\mathbf{f}, \text{ then } \boldsymbol{\sigma} = \mathbf{E}\mathbf{A}\mathbf{u} \qquad (4)(5a)(5b)$$

Similarly, in the case of the stress method, the problem and the solutions take the forms,

$$\min\{\Pi\}, \text{ in which } \Pi = \frac{1}{2}\boldsymbol{\sigma}^{\mathbf{t}}\mathbf{E}^{-1}\boldsymbol{\sigma} \text{ subject to } \mathbf{B}\boldsymbol{\sigma} = \mathbf{f} \quad \vdots \quad \boldsymbol{\sigma} = \mathbf{S}(\mathbf{BS})^{-}\mathbf{f}, \text{ then } \mathbf{u} = \left((\mathbf{BS})^{-}\right)^{\mathbf{t}}(\mathbf{BS})^{-}\mathbf{f} \qquad (6)(7a)(7b)$$

In which $\mathbf{K}^{-}$ is the Moore-Penrose generalized inverse matrix of the matrix $\mathbf{K}$. The regular matrix $\mathbf{S}$ is given by the decomposition of $\mathbf{E} = \mathbf{S}\mathbf{S}^{\mathbf{t}}$.

In the case of the mixed-type method shown in Tanami [9], the equations of the problem take the forms,

$$\mathbf{G}_{\mathbf{linear}}\begin{Bmatrix}\mathbf{u}\\ \boldsymbol{\beta}'\end{Bmatrix} = (\mathbf{BS})^{-}\mathbf{f}, \text{ in which } \mathbf{G}_{\mathbf{linear}} = \left[(\mathbf{BS})^{\mathbf{t}} \vdots -\left(\mathbf{I}_{\mathrm{m}} - (\mathbf{BS})^{-}(\mathbf{BS})\right)\right] \qquad (8)$$

By using the relationship such as the equations of $\mathbf{S}\boldsymbol{\sigma}' = \boldsymbol{\sigma}$ and $\boldsymbol{\sigma}' = (\mathbf{BS})^{-}\mathbf{f} + \left(\mathbf{I}_{\mathrm{m}} - (\mathbf{BS})^{-}(\mathbf{BS})\right)\boldsymbol{\beta}'$, the mixed-type solution derived from the equation (8) takes the form,

$$\begin{Bmatrix}\mathbf{u}\\ \boldsymbol{\beta}'\end{Bmatrix} = \mathbf{G}_{\mathbf{linear}}{}^{-}(\mathbf{BS})^{-}\mathbf{f} = \begin{Bmatrix}\left((\mathbf{BS})^{-}\right)^{\mathbf{t}}(\mathbf{BS})^{-}\mathbf{f}\\ \mathbf{0}\end{Bmatrix} \qquad (9)$$

The displacement and the axial force due to the equation (9) have the same forms of the equations (7b) and (7a), respectively. For instance, the equation of (7b), which is derived from the stress method (or the mixed type method), is consistent in the corresponding equations of (5a) by the following translations,

$$(7\mathrm{b}) \Rightarrow \mathbf{u} = \left((\mathbf{BS})^{-}\right)^{\mathbf{t}}(\mathbf{BS})^{-}\mathbf{f} = \left((\mathbf{BS})(\mathbf{BS})^{\mathbf{t}}\right)^{-}\mathbf{f} = \left(\mathbf{B}\mathbf{S}\mathbf{S}^{\mathbf{t}}\mathbf{B}^{\mathbf{t}}\right)^{-}\mathbf{f} = \mathbf{K}^{-}\mathbf{f} \Rightarrow \text{the first term of } (5\mathrm{a}) \qquad (10)$$

Note that the second term in the equation (5a) is zero from the assumption that the condition for the existence of a solution of equation (4) must be satisfied.

3. Analysis in this paper

One finite deformation analysis can be done by the extension of the mixed-type method introduced simply by the equations of (8) and (9).

In the case of truss structure, the initial length $\mathbf{L}$ of truss-member is the function of the co-ordinates $\mathbf{x}$ of the corresponding nodal points as $\mathbf{L}(\mathbf{x})$. Then the constitutive equation (2) can express in the form,

$$\boldsymbol{\sigma}(\mathbf{x}) = (\mathrm{EA})_{\mathrm{const}} \left(\frac{\mathbf{l_o}}{\mathbf{L}(\mathbf{x})} - 1 \right) \tag{12}$$

On the other hand, the axial force is derived from the equation (3) in the form,

$$\boldsymbol{\sigma}(\boldsymbol{\beta}) = \mathbf{B}^{-}\,\mathbf{f} + \left(\mathbf{I}_{\mathbf{m}} - \mathbf{B}^{-}\mathbf{B}\right)\boldsymbol{\beta} \tag{12}$$

From the equations of (11) and (12), we can make the following equation,

$$\mathbf{g}(\mathbf{x}, \boldsymbol{\beta}) = \boldsymbol{\sigma}(\mathbf{x}) - \boldsymbol{\sigma}(\boldsymbol{\beta}) = \mathbf{0} \tag{33}$$

Note that the equation (13) is nonlinear and has a mixed-type style which is similar to the linear equation (8). By solving the nonlinear equation (13), the axial force is decided from substituting $\boldsymbol{\beta}$ into the equation (12). The initial shape and the initial length of members are decided from $\mathbf{x}$ and $\mathbf{L}(\mathbf{x})$.

The numerical analysis of the equation (13) can be done by using the Newton-Raphson method in the form,

$$\mathbf{G}\begin{pmatrix} \Delta\mathbf{x} \\ \Delta\boldsymbol{\beta} \end{pmatrix} = (-\mathbf{g}) \tag{44}$$

In which,

$$\mathbf{G} = [\mathbf{G}_{\mathbf{x}} : \mathbf{G}_{\boldsymbol{\beta}}] = \left[\frac{\partial \mathbf{g}}{\partial \mathbf{x}} : \frac{\partial \mathbf{g}}{\partial \boldsymbol{\beta}} \right], \qquad \mathbf{G}_{\boldsymbol{\beta}} = \frac{\partial \mathbf{g}}{\partial \boldsymbol{\beta}} = -\left(\mathbf{I}_{\mathbf{m}} - \mathbf{B}^{-}\mathbf{B}\right) \tag{55)(16}$$

The full-rank rectangular matrix $\mathbf{G}$ has the size of $(\mathrm{m}, \mathrm{n}+\mathrm{m})$. Then, the convergent solution can be derived from the following iterative manner,

$$\begin{pmatrix} \mathbf{x} \\ \boldsymbol{\beta} \end{pmatrix} \Leftarrow \begin{pmatrix} \mathbf{x} \\ \boldsymbol{\beta} \end{pmatrix} + \mathbf{G}^{-}(-\mathbf{g}) \quad , \text{where } \mathbf{G}^{-} = \mathbf{G}^{\mathbf{t}}\left(\mathbf{G}\mathbf{G}^{\mathbf{t}}\right)^{-1} \tag{67}$$

4. Examples

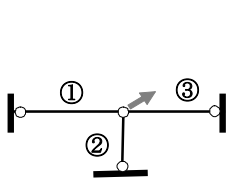

$$\mathbf{B} = \begin{bmatrix} 1 & 0 & -1 \\ 0 & 1 & 0 \end{bmatrix} \quad \mathbf{S} = \frac{1}{2}\begin{bmatrix} \sqrt{2} & 0 & 0 \\ 0 & 2 & 0 \\ 0 & 0 & \sqrt{2} \end{bmatrix}$$

$$\mathbf{B}^{-} = \frac{1}{2}\begin{bmatrix} 1 & 0 \\ 0 & 2 \\ -1 & 0 \end{bmatrix} \quad \mathbf{I} - \mathbf{B}^{-}\mathbf{B} = \frac{1}{2}\begin{bmatrix} 1 & 0 & 1 \\ 0 & 0 & 0 \\ 1 & 0 & 1 \end{bmatrix}$$

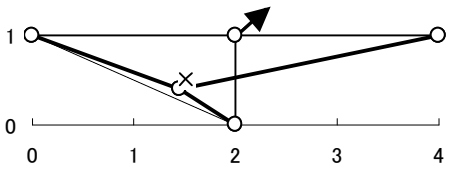

(a) Equilibrium shape of three-members plane truss (b) Initial shape as convergent solution

Figure 3: Example 1

Figure 3(a) shows the equilibrium shape with the lengths of three members of $l_1 = l_3 = 2$, $l_2 = 1$ under the load condition of $f_x = f_y = 0.5$ together with the components of matrices $\mathbf{B}$ and $\mathbf{S}$. The value of the notation of $(\mathrm{EA})_{\mathrm{const}}$ in the equation (11) which means the product of the area of cross-section and the Young's modulus is one in this example at each member. Then the unit load means that the load becomes in the real value of $(\mathrm{EA})_{\mathrm{const}}$. After a few times of the repetitions in the equation (17), both the convergent solutions of $\boldsymbol{\beta} = (\beta_1, \beta_2, \beta_3)$ and $\mathbf{x} = (x_1, y_1)$ take the forms,

$$(0.01502,\ 0.\ ,\ 0.01502) \quad \text{and} \quad (1.458,\ 0.3882) \tag{78)(19}$$

Then,

$$\mathbf{L} = (1.581,\ 0.6667,\ 2.615) \text{ and } \boldsymbol{\sigma} = (0.2649,\ 0.5000,\ -0.2350) \tag{20)(21}$$

The bold real lines in the figure 3(b) show the initial shape given by the equation (19). The mark x in the same figure is the first approximation point for getting the quick convergent solution of the iteration analysis which is estimated as the solution of the corresponding linear analysis. The dotted line connected between two supported points in the same figure implies one restriction imposed on this example to obtain the solution. The reason is that the total length of the corresponding two members can not be shorter than the length of the dotted line. One idea to clear this kind of the restriction condition is simply denoted by the following example.

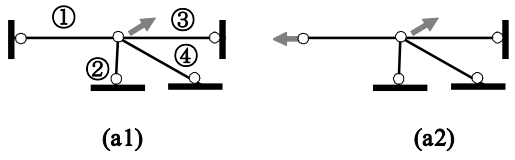

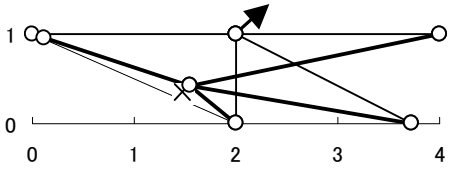

(a1) Equilibrium shape of four-members stable truss

(a2) Equilibrium shape of four-members unstable truss (b) Initial shape of (a2)

Figure 4: Example 2

Figure 4 is one example where the equilibrium shape composed of four members shown in the Figure 4(a1) can not have the corresponding initial shape under the load of $f_x = f_y = 0.6$ due to the restriction condition. Then we can try to make the equivalent structure such as the Figure 4(a2) by replacing one supported point by one free nodal point. Then all the same analysis presented in the first example to the new unstable truss structure can be carried out to take the initial shape shown in the Figure 4(b).

6. Conclusion

I know it is difficult to say about the advantages of the analysis in this paper from the results obtained by the examples which are too simple to summarize the conclusive remarks. But I can say that the mixed-type analysis has a merit under the condition that equilibrium shape is given as constant.

References

[1] Tanaka H. and Hangai Y. Rigid body displacement and stabilization conditions of unstable truss structures, Proceedings of IASS, 1986;55-62.

[2] Tanami T. Explicit solution form of stress and displacement of structures with/without mechanism, Proceedings of IASS, 1997;(2)811-814.

[3] Tanami T. Structural analysis based on the existence condition of solution, Proceedings of 6th APCS, 2000;(ll)801-808.

[4] Tanami T. Structural analysis based on condition for existence of solution, J. Struct. Constr. Eng., AIJ, 2001; no.547 91-96(in Japanese)

[5] Tanami T. Solution form available to any structural analysis also with singularity, Proceedings of IASS, Nagoya, 2001;

[6] Tanami T. A shape-finding analysis by residual of equilibrium equation as a linear problem, Proceedings of IASS, Romania, 2005;(l)151-154.

[7] Tanami T. Structural analysis based on condition for existence of solution(Stress method and analysis of tension structures), J. Struct. Constr. Eng., AIJ, 2006; no.610 85-90(in Japanese)

[8] Tanami T. One of the simple analyses of cable-net structures, International Symposium on New Olympics New Shell and Spatial Structures, IASS-APCS 2006 Beijing China, Extended Abstracts 126-127.

[9] Tanami T. Structural analysis based on condition for existence of solution(Decision of initial shape and stress from equilibrium shape), J. Struct. Constr. Eng., AIJ, 2008; Vol.73 no.625 399-40490(in Japanese)

Proceedings of the 6th International Conference on
Computation of Shell and Spatial Structures
IASS-IACM 2008: "Spanning Nano to Mega"
28-31 May 2008, Cornell University, Ithaca, NY, USA
John F. ABEL and J. Robert COOKE (eds.)

Mistakes and paradoxes in solutions of spatial, geometrically nonlinear problems and equilibrium stability problems

* Anatoly PERELMUTER, Vladimir SLIVKER

*SCAD Soft, Kiev, Ukraine
avp@scadsoft.com

Abstract

The object of consideration comprises geometrically nonlinear (second-order) problems and equilibrium stability problems for spatial bar structures. Unlike that in planar problems, the matrix of geometric stiffness for particular bars here depends both on the longitudinal forces *and* the distribution of the bending and torsion moments. Besides that, a traditional point of view becomes erroneous: that the components of an ordinary moment vector can be used as generalized forces that correspond to the slope components in the structure's nodes.

1. Introduction

It is a well-known fact that equilibrium stability problems are a peculiar category of structural mechanics problems, so they feature both complexity and an especially "cunning" nature that provoke erroneous results in calculations. A particularly special subcategory of those comprises geometrical nonlinearity (second-order problems) and stability of equilibrium of spatial structures that contain bar members. The first thing to do about those problems is to pay more attention to an expression of elementary work of a moment load applied to a perfectly rigid body, even in the case when the moment load originates from conservative forces. The matter is that the behavior of a moment load depends very much on how it is exactly applied. A strict mathematical analysis (Ispolov and Slivker [2]) shows that, when slopes in a system are big, the generalized forces conjugated to the slopes are so-called generalized moments (or *L*-moments). The general geometrically nonlinear theory uses the following correct formula for the generalized moments vector $\boldsymbol{L}$,

$$\boldsymbol{L} = \frac{\sin\varphi}{\varphi}\boldsymbol{M} + \frac{1-\cos\varphi}{\varphi^2}\boldsymbol{M}\times\boldsymbol{\varphi} + \frac{\varphi-\sin\varphi}{\varphi^3}(\boldsymbol{M}\cdot\boldsymbol{\varphi})\boldsymbol{\varphi}\,, \tag{1}$$

where $\boldsymbol{M}$ is an ordinary moment vector, $\boldsymbol{\varphi}$ is a full slope vector, and φ is the latter's absolute value. The second-order theory makes a much simpler expression of that, so the generalized moments vector becomes $\boldsymbol{L} = \boldsymbol{M} + \frac{1}{2}\boldsymbol{M}\times\boldsymbol{\varphi}$. It is easy to notice that any difference disappears between the generalized and ordinary moments (see the table below) in linear problems as well as in nonlinear but two-dimensional ones. However, it is not the case in three-dimensional problems.

Problems	Linear	Nonlinear
2D	$\boldsymbol{L}=\boldsymbol{M}$	$\boldsymbol{L}=\boldsymbol{M}$
3D	$\boldsymbol{L}=\boldsymbol{M}$	$\boldsymbol{L}=\boldsymbol{M}+\frac{1}{2}\boldsymbol{M}\times\boldsymbol{\varphi}$

As it can be seen in the table, it is three-dimensional nonlinear problems where there appears an additional term in the generalized moments so that they become different from the ordinary *M*-moments. The presence of those additional terms entails some peculiarities in formulations of problems related to stability of equilibrium of spatial bar structures. An important issue should be noted in relation to the notion of a generalized moment. According to the general variational principle of virtual displacements, those of equilibrium equations that correspond to the rotation (slope) vector components are equations of balance not between the ordinary

moments but between the generalized moments. This is especially important in formulation and (or) interpretation of moment boundary conditions because in 3D problems those are conditions not for the ordinary moments but for *L*-moments. Ignoring this circumstance may produce a totally mistaken mathematical formulation of a mechanical problem.

2. On a variational formulation of spatial stability problems

A general mathematical formulation of the linearized problem of equilibrium stability becomes a generalized eigenvalue problem after it has been converted into a discrete form: $(\boldsymbol{R}_0 - \lambda \boldsymbol{G})\boldsymbol{q} = 0$, where $\boldsymbol{R}_0$ is an initial stiffness matrix of the system; $\boldsymbol{G}$ is a geometric stiffness matrix, $\boldsymbol{q}$ is a vector of bifurcation displacements. After the problem has been converted into a discrete form using some known method, the further solution is quite obvious. The issue is not the method of discretization but a correct form of the equilibrium stability functional, S, which is the basis for the discretization procedure. The general form of the functional is known in the theory of elasticity; it is a Brian–Trefftz functional. However, the functional needs some adjusting to the three-dimensional bar theory because the mechanical model of a bar itself contains a set of perfectly rigid bodies: any cross-section of a classic Bernoulli–Euler bar is a rigid body. This circumstance being allowed for, we can build correct forms of the equilibrium stability functionals for 3D bars. We are not doing it here for the lack of space, instead just referring to our recently published book, Perelmuter and Slivker [3]. However, some of the functionals for particular problems that we have derived will be given below as examples. The examples (intentionally simple enough) will demonstrate clearly what unexpected results some stability analyses can produce.

3. Some examples

3.1 Example 1

The object of consideration is a stability of equilibrium of a stand-alone node constrained rigidly against rotation about the *X* axis and constrained in an elastic fashion against rotation about the other two axes. The stiffness factors of the elastic constraints imposed on the node are denoted by γ_y and γ_z, respectively. Let an external moment *M* be produced by two force couples as shown in Fig. 1-*a*.

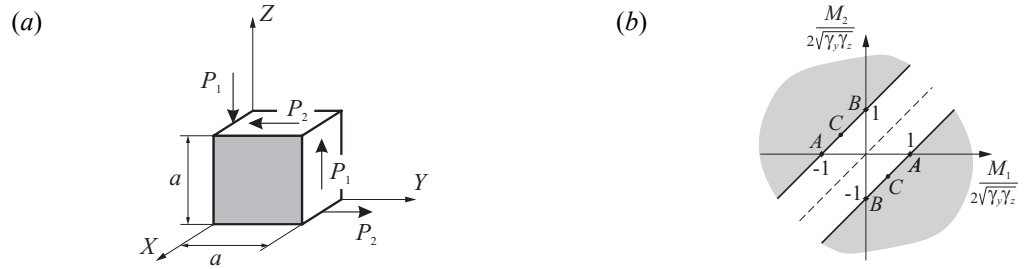

Figure 1: Stability of equilibrium of a stand-alone node

Even this seemingly simplest of problems is somewhat sophisticated, though this fact may be missed at a first glance. The correct expression for the equilibrium stability functional is

$$\mathsf{S} = \frac{\gamma_y}{2}\theta_y^2 + \frac{\gamma_z}{2}\theta_z^2 + (M_2 - M_1)\frac{\theta_y \theta_z}{2} \tag{2}$$

An analysis of this functional (a quadratic form) shows that the area of equilibrium stability in the coordinate plane of dimensionless load parameters (Fig. 1-*b*) is an infinite strip with equal slopes to both coordinate axes. Note that the points C of the stability area's boundary conform to two mutually annulling moments applied to the node. In simple words, the node is seemingly unloaded but capable of losing its equilibrium stability. At the same time, a dash line that conforms to a semi-tangential moment applied to the node never gets to the boundary of the equilibrium stability area.

3.2 Example 2

A classic Greenhill problem is under consideration: stability of a cantilever bar under a torque. Our generalization of the Greenhill problem is to consider 5 different versions of the external moment created by dead force couples (Fig. 2). The difference lies in the orientation of arms of the forces.

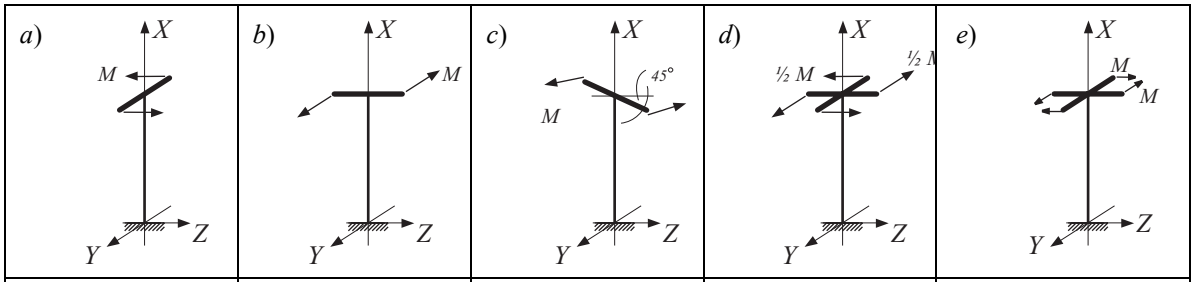

$\frac{\pi E\sqrt{I_y I_z}}{2l}$	$\frac{\pi E\sqrt{I_y I_z}}{2l}$	$\frac{\pi EI}{2l}$	$\frac{\pi E\sqrt{I_y I_z}}{l}$	$\frac{E\sqrt{I_y I_z}}{l}$

Figure 2: A generalized Greenhill problem

A correct expression of the S functional for this problem in standard designations is

$$\mathsf{S} = \frac{1}{2}\int_0^l \left[EI_z v''^2 + EI_y w''^2 + M(w'v'' - w''v') \right] dx - \frac{1}{2}\delta^2\Pi_M \tag{3}$$

where $\delta^2\Pi_M$ is second variation of the moment load's potential. Formulae for the critical moments derived from the stationarity conditions for the functional (3) are given at the bottom of Fig. 2. It turns out a quasi-tangential external moment is twice as dangerous as a semi-tangential external moment from the standpoint of stability. Curiously, a couple of mutually annulling moments produces a least stable load case.

3.3 Example 3

A Prandtl–Mitchell–Timoshenko problem is under consideration: stability of a cantilever bar in planar bending (Fig. 3).

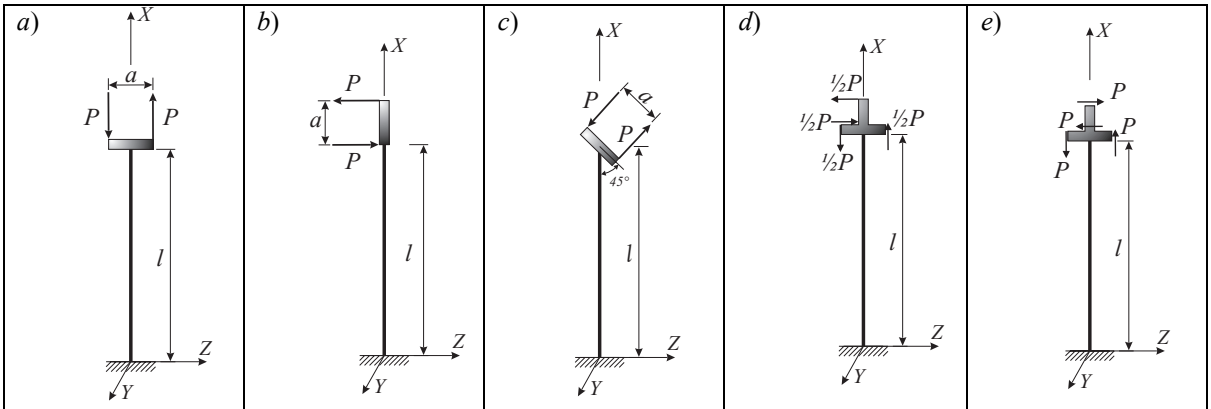

$\frac{\pi\sqrt{GI_x EI_z}}{2l}$	$\frac{\pi\sqrt{GI_x EI_z}}{2l}$	$\frac{1.34\sqrt{GI_x EI_z}}{l}$	$\frac{\pi\sqrt{GI_x EI_z}}{l}$	$\frac{\sqrt{GI_x EI_z}}{l}$

Figure 3: A generalized Prandtl–Mitchell–Timoshenko problem

Formula (4) gives a general expression of the equilibrium stability functional for the problem:

$$\mathsf{S} = \frac{1}{2}\int_0^l \left[GI_x \theta_x'^2 + EI_z v''^2 + 2M\theta v'' \right] dx - \frac{1}{2}\delta^2\Pi_M \tag{4}$$

This report seems to be the first time when a correct expression for the S functional of this problem is used. Expressions of the critical external moment value in all load cases are given by formulas at the bottom of Fig. 3. The case in Fig. 4 is obviously a generalization of the preceding five load cases. The same figure shows an area of equilibrium stability for the problem, constructed in dimensionless load parameters. The figure also describes designations and gives an equation that determines the boundary of the equilibrium stability area.

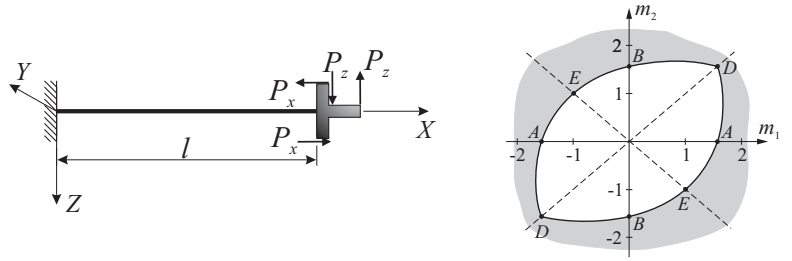

$$M_1 = P_x a\,, \quad M_2 = P_z a\,,$$

$$m_1 = \frac{M_1 l}{\sqrt{EI_z GI_x}}\,, \quad m_2 = \frac{M_2 l}{\sqrt{EI_z GI_x}}\,,$$

$$\cos(m_1 + m_2) = \frac{2m_1 m_2}{m_1^2 + m_2^2}\,.$$

Figure 4: An equilibrium stability problem in bending of a bar by two external moments

Here is a detailed expression of the stability functional for the problem in Fig. 4:

$$\mathsf{S} = \frac{1}{2}\int_0^l \left[GI_x \theta_x'^2 + EI_z v''^2 - 2(M_1 + M_2)\theta_x' v' \right] dx + (M_1 + M_2)\theta_x(l)v'(l) \underline{- M_1 \theta_x(l)v'(l)}\,.$$

The underlined term is second variation of the moment load's potential. As it can be seen in Fig. 4, the stability area is a lens-like shape with an angular point (point D). The presence of the angular point proves the critical load to be a multiple one. Hence, the critical value of the external semi-tangential moment conforms to two linearly independent modes of buckling. By the way, the fact that the critical load is different here than that for the problems in Figs. 3-*a*, 3-*b*, on one hand, and in Fig. 3-*d*, on the other hand, has been confirmed by an experiment conducted at our request. That experiment has shown also both the calculated critical load and the experimentally measured one are the same.

4. On myths and paradoxes in 3D stability

It was noticed over twenty-five years ago (by Argyris [1]) that three-dimensional geometrically nonlinear problems entail issues that had never been noticed earlier in two-dimensional problems. He noted that the equilibrium equations written in moments produce an asymmetric matrix, and this is seemingly in contradiction with the variational formulation of the problem. Therefore he suggested that internal bending moments in bars should have been treated as semi-tangential. This arbitrariness in modeling could not satisfy sophisticated mechanics scientists. Further attempts to avoid contradictions arising in the theory gave birth to a lot of myths and false beliefs, which were discussed in the literature on the subject many times. The actual basis for all those myths is a stubborn wish to treat ordinary moments as generalized forces (similarly to what Argyris did) followed by trying hard to find such generalized displacements that would be conjugated in energy to the ordinary moments. We have managed to give a proof that the attempts like those cannot produce any good result. All contradictions will disappear from the theory if the problem is formulated the other way around: we take the slope vector as generalized displacements and then find that its conjugate generalized force is an *L*-moment introduced by us.

5. Basic results

(1) Functionals from a linearized formulation of the elastic equilibrium stability have been generalized onto the case of an elastic body with perfectly rigid bodies incorporated in it.
(2) A new force or load notion has been added to the theory of mechanics – a generalized moment vector (an ***L***-moment).
(3) Correct forms of the equilibrium stability functionals for spatial bars have been derived.

References

[1] Argyris J.H. An excursion into large rotations. *Comp. Meth. Appl. Mech. Engng.* 1982; **32**:85-155.

[2] Ispolov Y.G., Slivker V.I. On a conservative moment load (in Russian). *Structural Mechanics and Analysis of Constructions* 2007; **1**:61-67.

[3] Perelmuter A.V., Slivker V.I. Structural equilibrium stability and related problems (in Russian). Vol.1. Moscow, 2007, Scadsoft Publishing.